Electronic Supplementary Material (ESI) for Journal of Materials Chemistry A.

Impact of Iron-Nitride-encapsulated Bimetallic Nickel Molybdenum Nitrides on Water-Splitting Efficiency in Alkaline Electrolytes

Venkatesan Jayaraman, Ganghyun Jang, Gi-Hyeok Noh, Manasi Murmu, Do-Heyoung Kim*

School of Chemical Engineering, Chonnam National University, 77 Yongbong-ro, Gwangju 61186, Republic of Korea

Keywords: Interstitial nitride; Interface modulation; Water splitting; Active site, Electrolyte diffusion

***Corresponding author**

Prof. Do-Heyoung Kim

E-Mail: **kdhh@chonnam.ac.kr**

Calculations details for Tafel, C_{dl}, ECSA, TOF, and number of active sites

For the intrinsic electrochemical activity enhancement assessment and to analyze the rate determination steps in HER and OER Tafel slop has been used. For these measurements the following Tafel equation was used[1].

$$\eta = a + b \log |j|$$

where, *η, b, and j* denotes the overpotential, Tafel slope, and current density respectively.

In general the double layer capacitance of the electrodes are used for the calculation of electrochemical active surface area. The double layer capacitance Cdl has been calculated by slop of the linear regressions of anodic (ia) and cathodic (ic) current density with respect to scan rate in the non-faradic region. The double layer capacitance can be calculated from the following equation[1].

$$i_a = \upsilon C_{dl}$$

Then, the appropriate electrochemical active surface area (ECSA) vales were calculated by the following formula.

$$ECSA = C_{dl}/C_s$$

In which, the Cs-the specific capacitance (40 mF cm-2 for 1.0 M KOH), C_{dl}-calculated double layer capacitance.

The ECSA normalized polarization curves for both HER and OER activity has been calculated by the following formula[1].

$$\text{Specific activity} = j/ECSA$$

Where j- is the observed current density [2].

Turnover frequency (TOF) of the electrodes were calculated based on the previously reported method [1, 3-5].

$$TOF = \frac{Total\ Hydrogen\ Turnovers/cm^2\ of\ geometric\ area}{No.\ of\ Surface\ active\ sites\ /cm^2\ of\ geometric\ area}$$

The prepared electrode consists of four different elements with different phases of the material. The exact elemental quantity and its ratios in the electrode are unknown. It is difficult to quantify the molar ratios of the elements in the electrode very precisely. Since, the ratio is an unknown, the reported articles suggest to calculate the number of electrons consumed by the surface of the electrodes to estimate the number of active sites. The total number of hydrogen turnovers assessed for the observed current density of the electrode by the following equation[1, 5]:

$$Number\ of H_2 = \left(j\frac{mA}{cm^2}\right)\left(\frac{1C\ s^{-1}}{1000\ mA}\right)\left(\frac{1\ mol\ e^-}{96485.3\ C}\right)\left(\frac{1\ mol\ H_2}{2\ mol\ e^-}\right)\left(\frac{6.022\ \times 10^{23}\ H_2\ molecules}{1\ mol\ H_2}\right)$$

$$= 3.12\ \times 10^{15}\ \frac{H_2/s}{cm^2}\ per\ \frac{mA}{cm^2}$$

The total number of oxygen turnovers of the electrodes was estimated for the perceived current density of the electrodes using the following equation[1, 5]:

$$Number\ of\ O_2 = \left(j\frac{mA}{cm^2}\right)\left(\frac{1C\ s^{-1}}{1000\ mA}\right)\left(\frac{1\ mol\ e^-}{96485.3\ C}\right)\left(\frac{1\ mol\ O_2}{4\ mol\ e^-}\right)\left(\frac{6.022\ \times 10^{23}\ O_2\ molecules}{1\ mol\ O_2}\right) =$$

$$1.56\ \times 10^{15}\ \frac{O_2/s}{cm^2}\ per\ \frac{mA}{cm^2}$$

Calculation of Surface-Active Sites

The electrons consumed by the electrode surface is calculated by using reduction peak are integration (Q) with the following expression[1, 4]:

$$Q = \frac{\int I \, dV}{v}$$

where Q the quantified charge carriers available over the surface of the electrodes, which is associated with the area of the reduction peak respect to scan rate over the defined potential window. For this present work, it is assumed that the surface redox reactions are single electron transfer reactions (Fe, Ni are considered as an active sites with Mo is playing a supporting role). From the quantified charge carriers, further the number of surface-active sites (N_A) was calculated as follows

$$N = \frac{Q}{q}$$

Where, $q = 1.602 \times 10^{-19}$ C[1].

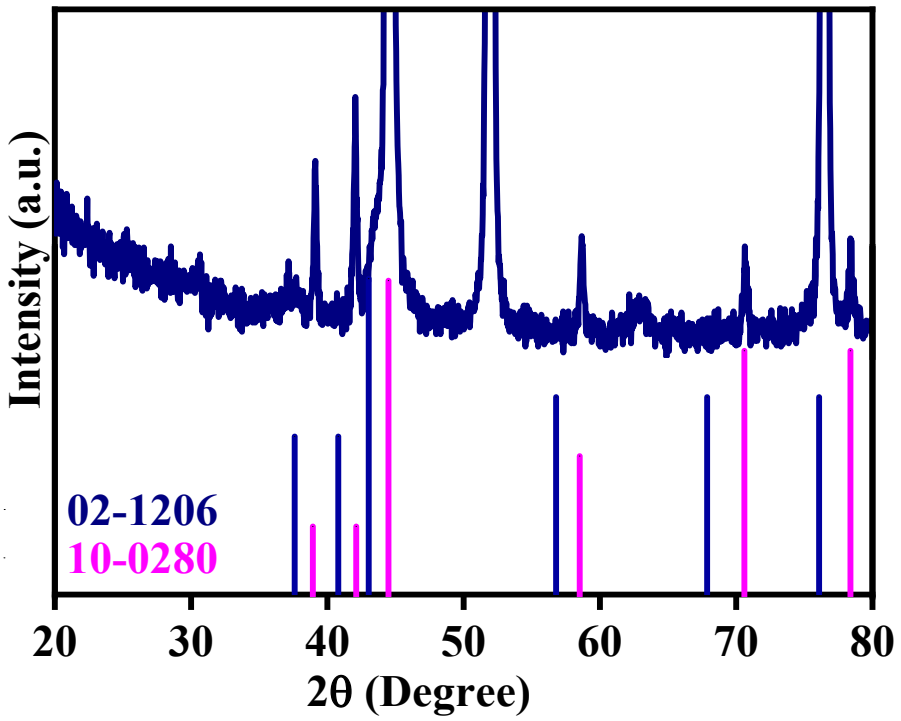

Figure S1-XRD Analysis of in-situ grown iron nitride on Ni Foam

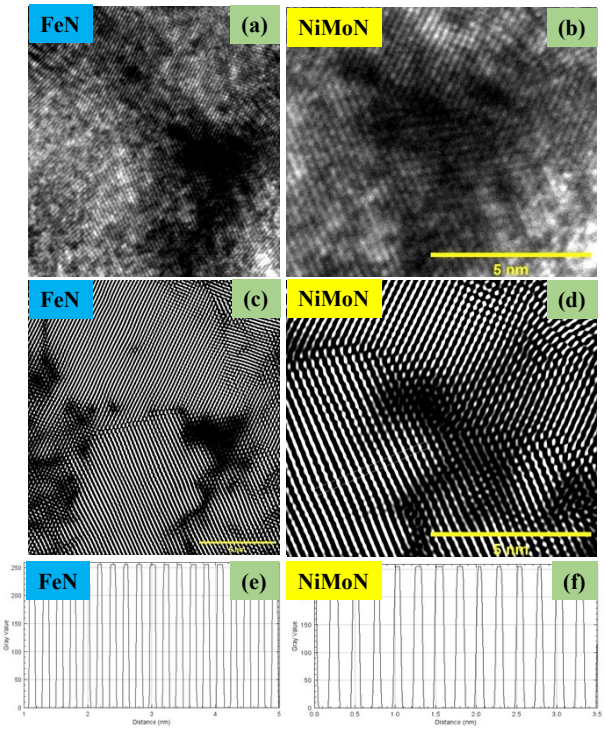

Figure S2 HRTEM analysis of the sample (a,c,e) releated to Iron nitride (b,d,f) corresponding to the NiMoN Phases from the 1FeNiMoN sample.

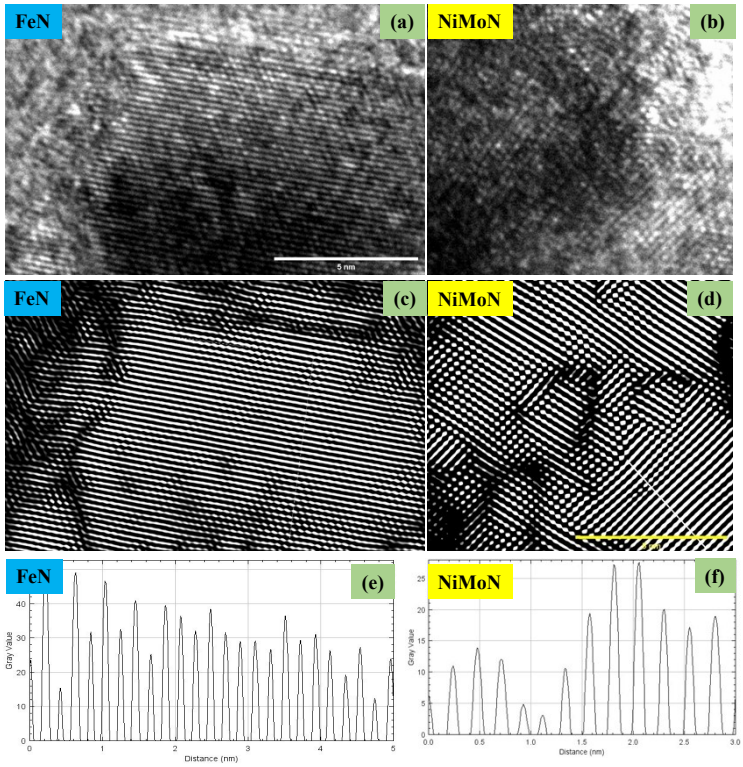

Figure S3 HRTEM analysis of the sample (a,c,e) releated to Iron nitride (b,d,f) corresponding to the NiMoN Phases from the 3FeNiMoN sample.

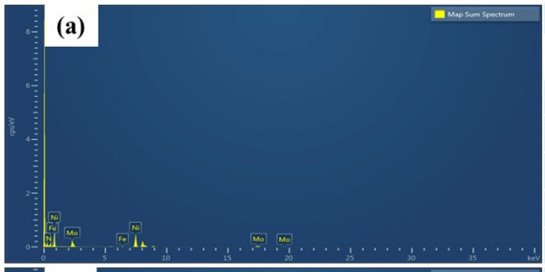

Element (b)	Line Type	k Factor	Wt%	Wt% Sigma	Atomic %
N	K series	3.530	2.80	2.40	12.11
Fe	K series	1.136	1.52	0.45	1.64
Ni	K series	1.151	64.56	2.90	66.60
Mo	K series	4.432	31.12	2.65	19.64
Total:			100.00		100.00

Element (d)	Line Type	k Factor	Wt%	Wt% Sigma	Atomic %
N	K series	3.487	5.33	0.58	21.36
Fe	K series	1.159	3.62	0.19	3.63
Ni	K series	1.179	58.71	0.80	56.10
Mo	K series	4.672	32.34	0.81	18.91
Total:			100.00		100.00

Figure S4 EDS Analysis (a-b) 1FeNiMoN, (c-d) 3FeNiMoN samples of the electrodes

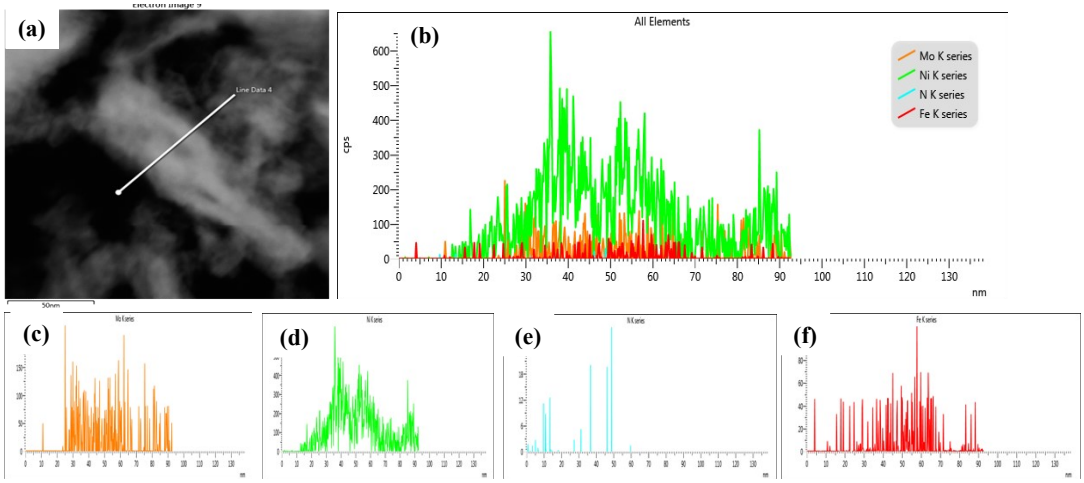

Element (h)	Line Type	k Factor	Absorption Correction	Wt%	Wt% Sigma	Atomic %
N	K series	3.530	1.00	1.64	2.40	7.40
Fe	K series	1.136	1.00	2.41	0.48	2.73
Ni	K series	1.151	1.00	64.09	2.78	68.91
Mo	K series	4.432	1.00	31.85	2.52	20.96
Total:				100.0		100.0

Figure S5 EDS line Profile and quantification of the elements in the 1FeNiMoN sample

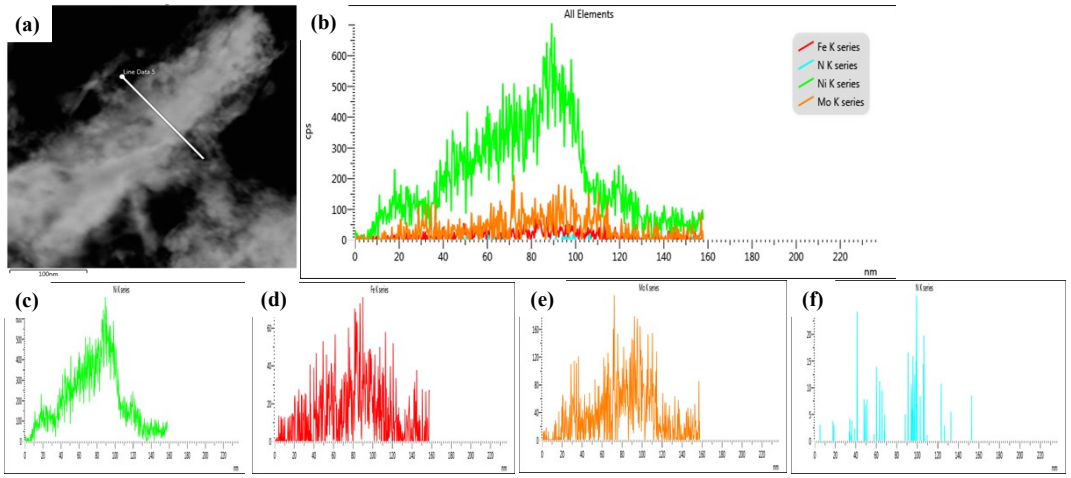

Element (h)	Line Type	k Factor	Absorption Correction	Wt%	Wt% Sigma	Atomic %
N	K series	3.487	1.00	6.53	0.73	25.55
Fe	K series	1.159	1.00	3.50	0.21	3.43
Ni	K series	1.179	1.00	54.30	0.90	50.66
Mo	K series	4.672	1.00	35.67	0.93	20.36
Total:				100.00		100.00

Figure S6 EDS line Profile and quantification of the elements in the 3 FeNiMoN sample

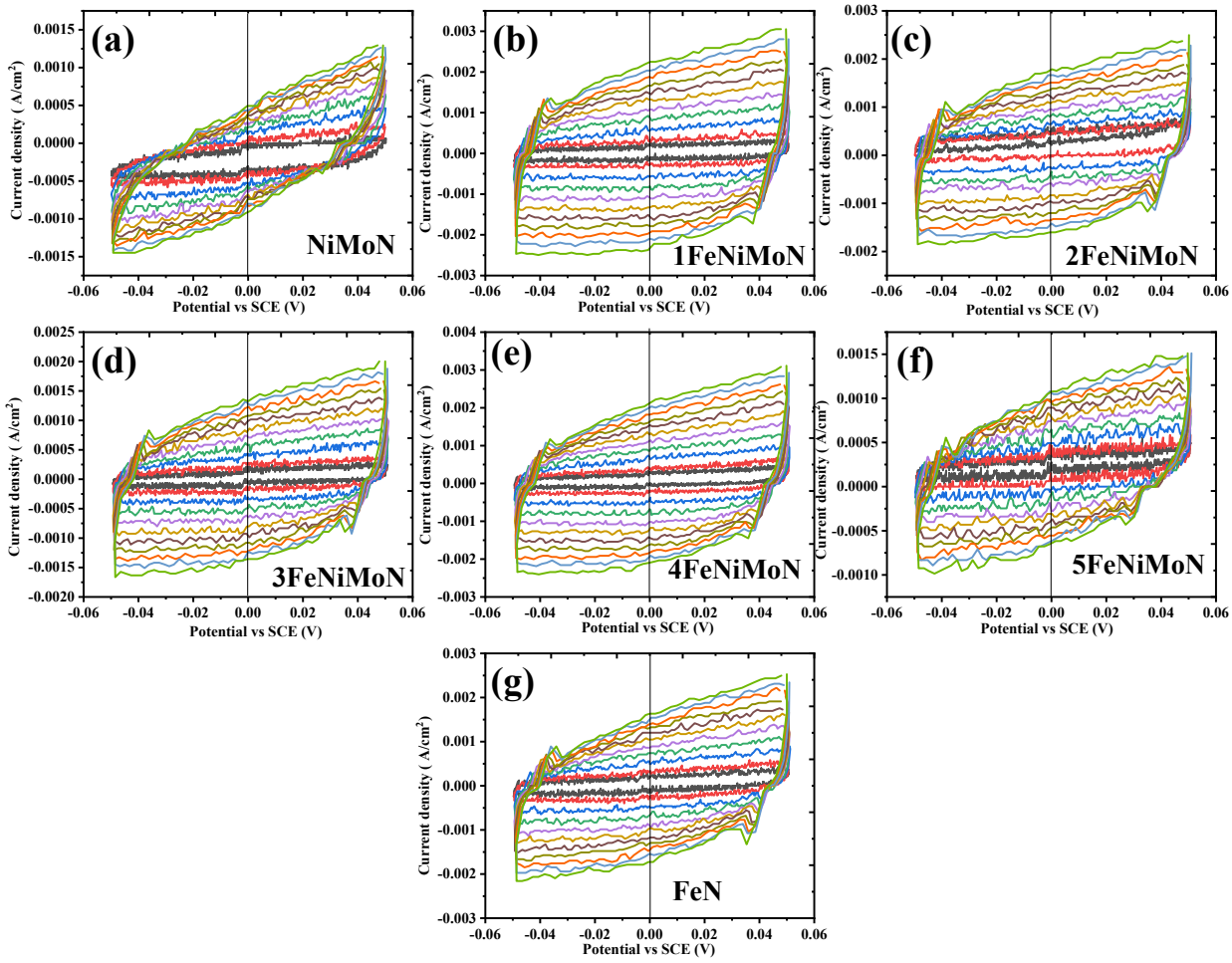

Figure S7. CV measurement of the samples with different scan rate in the non-faradiac region for the OER analysis

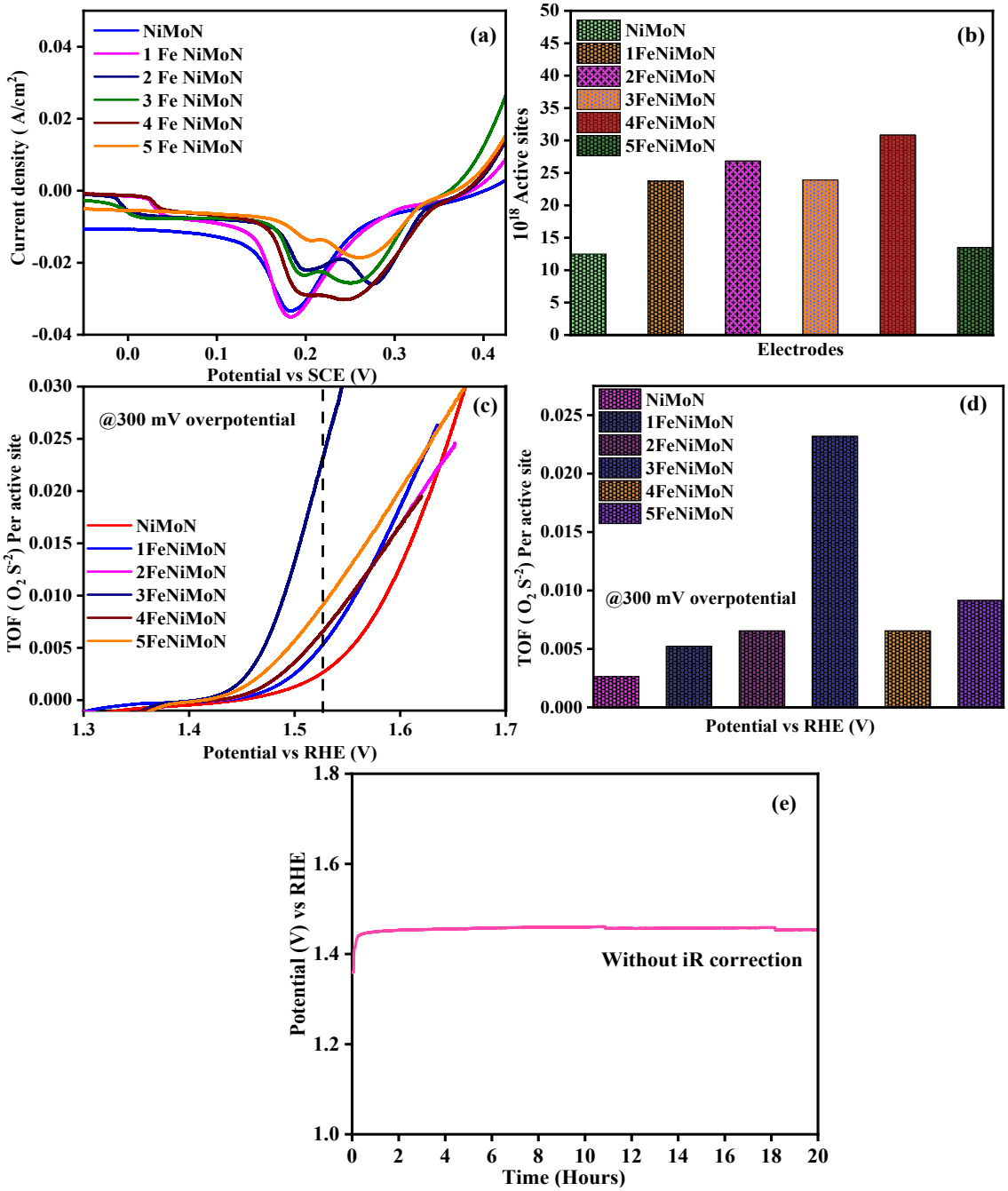

Figure S8. (a) Reduction area integration for the calculation of the number of active sites, (b) calculated number of active sites of the electrodes, (c) Measured TOF of the electrodes for the OER analysis, (d) Comparaion of calculated TOF value at 300 mV overpotential for the prepared electrodes, (e) OER stability analysis without iR correction.

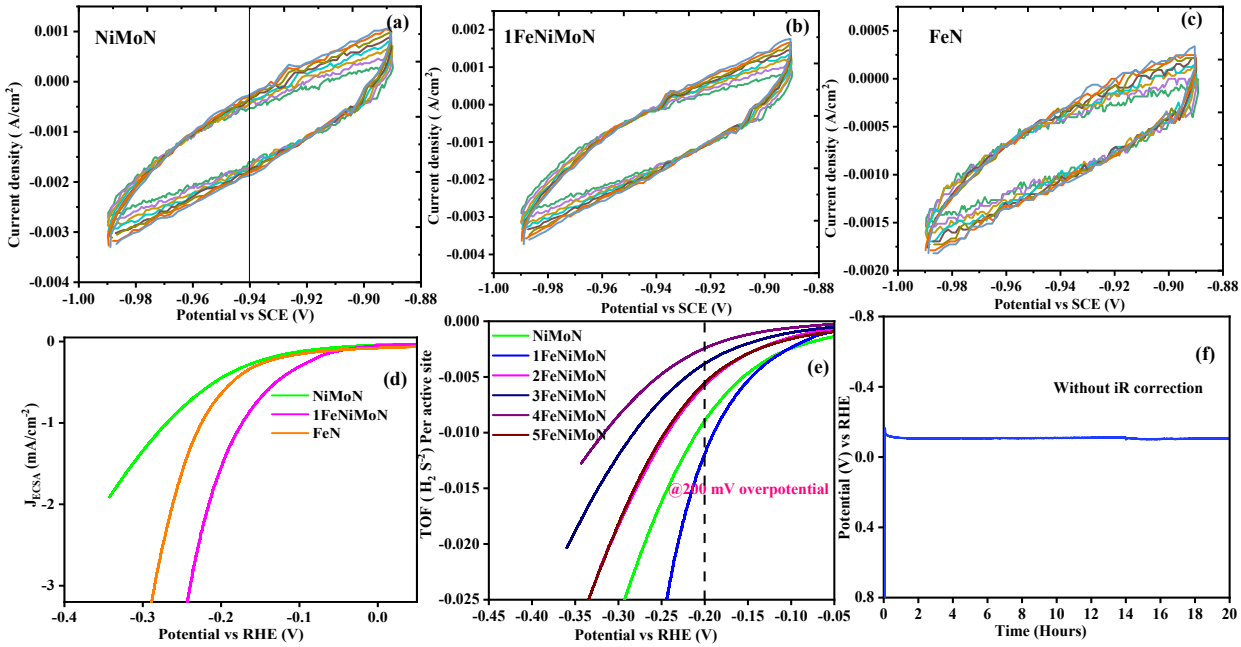

Figure S9. (a-c) CV measurement with different scan rate in the non-faradic region for the calculation of C_{dl} of the HER region (d) ECSA normalised HER activity of the samples, and (e) Calculated TOF of the prepared electrodes, (f) HER stability analysis without iR correction.

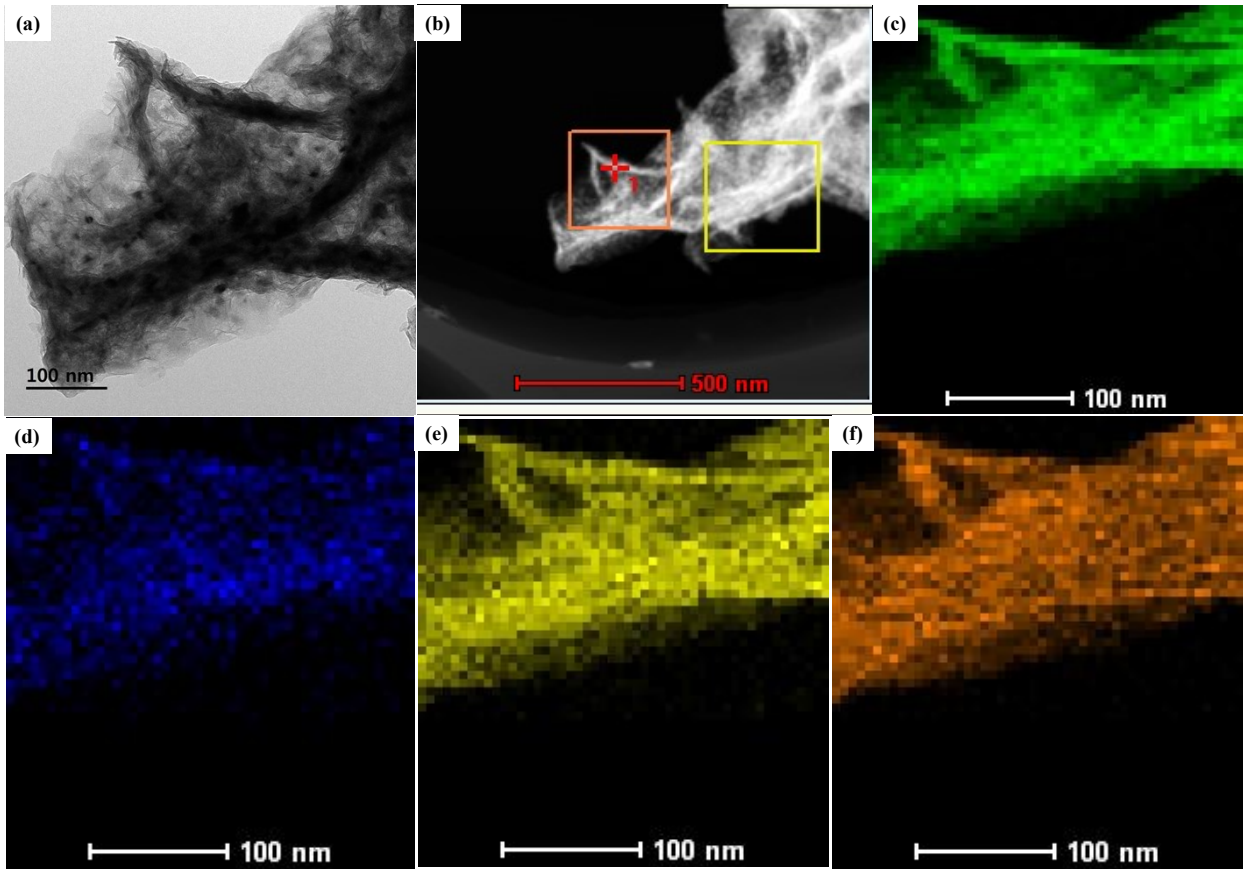

Figure S10. Post stability analysis of 3FeNiMoN (a) TEM Analalysis (b) EDS Analysis (c) Ni, (d) Mo, (e) Fe, and (f) N elements

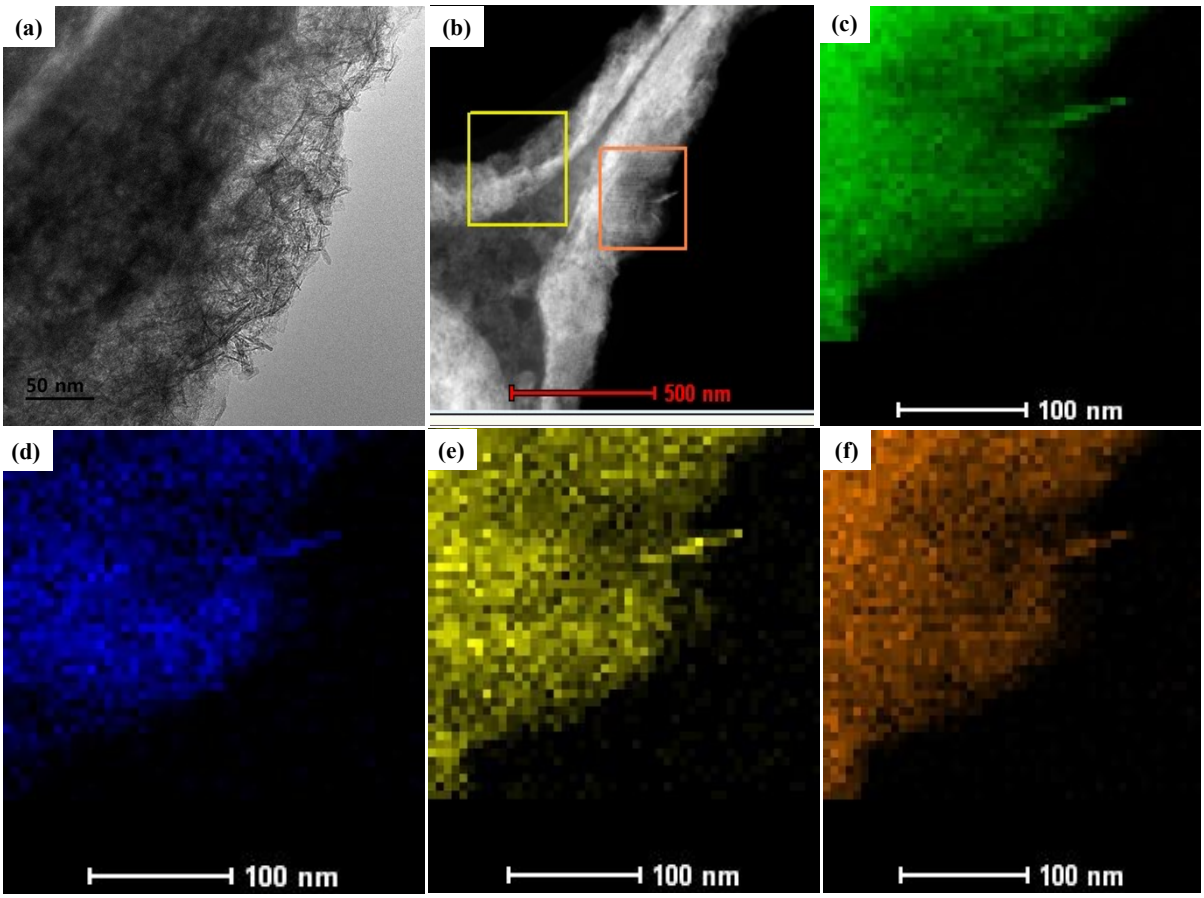

Figure S11. Post stability analysis of 1FeNiMoN (a) TEM Analalysis (b) EDS Analysis (c) Ni, (d) Mo, (e) Fe, and (f) N elements

Table S1-Binding energy position of elements in the 1FeNiMoN and 3FeNiMoN

Name	Ni 2p Binding energy (eV)						Mo 3d Binding energy (eV)				N 1s Binding energy (eV)			Fe2p Binding energy (eV)					
1FeNiMoN	852.58	854.48	859.98	871.08	873.08	878.98	227.88	230.88	231.38	234.28	393.68	396.18	398.08	710.38	713.48	718.58	723.58	726.98	732.38
3FeNiMoN	852.18	855.48	861.18	869.58	873.38	879.88	228.88	231.68	232.28	235.08	394.48	396.68	398.58	710.38	713.58	718.58	723.58	727.18	732.48

Table S2-ICP-OES Analysis of NiMoN, 1FeNiMoN, 3FeNiMoN samples

Sample	Element	Wavelength (nm)	Concentration (wt%)
NiMoN	Ni	231.604	87.4
	Mo	202.031	11.5
1FeNiMoN	Fe	238.204	0.21
	Ni	231.604	100
	Mo	202.031	5.68
3FeNiMoN	Fe	238.204	1.24
	Ni	231.604	92.6
	Mo	202.031	4.75

Table S3 BET measurements of the electrodes

Sample Name	BET Specific surface area ($m^2\ g^{-1}$)	Measured Pore volume ($cc\ g^{-1}$)	Measured Mean pore diameter (nm)
NiMoN	4.1253	0.049218	47.723
1FeNiMoN	2.4635	0.023036	37.404
3FeNiMoN	4.1508	0.037858	36.482

Table S4. The OER activity comparison of the optimized iron nitride/NiMoN with the literature.

Catalyst Name	Electrolyte Solution details	Current density ($mAcm^{-2}$)	Onset/ Overpotential mV (cm^{-2})	Tafel slope ($mV\ dec^{-1}$)	Ref
$NiSe_2$–NPs/NiMoN–NRs	1.0 M KOH	10	241	95.2	6
NiMoN-NF700	1.0 M KOH	50	290	54	7
Co_4N@CeO_2	1.0 M KOH	10, 100	263,325	60.9	8
CeO_2–Fe_2N/NFC_{-2}	1.0 M KOH	10	266	78.1	9
Fe_7S_8/Fe_2N	1.0 M KOH	10	220	38.3	10
W_2N_3/Fe_2N	1.0 M KOH	50, 100	268.5, 285.9	59.3 mV	4
NiO@$CuCo_2O_4$/MoNi	1 M KOH	50	313.0	69	11
$NiCo_2O_4$/MoO_2@ALD-NiO	1 M KOH	100		57	12
Co_3N–$Mo_{0.2}$@FeOOH/NF	1 M KOH	50, 100	250, 260	48	13
Mo_2N/NiS-5:1	1.0 M KOH	10, 30	298, 391	181.85	14
Ir-Ni_3N	1 M KOH	1, 10	248.16 , 273.30	34.01	15
Co-Mo-N	1.0 M KOH	10	288	95	16
NNS-d/Ni_2P@NC-NF	1 M KOH	10	210	44.2	17
$(Fe_{1-x}Cux)_4N$-Cu_2O/CF	1 M KOH	10	307	40	18
FeNi$(MoO_4)_x$@NF	1.0 M KOH	10, 1000	227, 351	47.51	19
CoFe-0.44	1.0 M KOH	10, 100	229, 281	64.2	20
Fe_2P/Ni_3N	1 M KOH	100	212	45.5	21
cRu-Ni_3N	1 M KOH	20	226	40.4	22
NiMoN	1 M KOH	10, 50, 100	270, 333, 368	92.26	This work
3FeNiMoN	1 M KOH	10, 50,100	202, 230, 247	41.72	This work

Table. S5 Calculated double layer capacitance, Electrochemical active surface area, solusion and charge transfer resistance values of the electrodes

Sample Name	2Cdl (mF/cm^2)		ECSA		R_S (Ω)		R_{CT} (Ω)	
	OER	HER	OER	HER	OER	HER	OER	HER
NiMoN	6.12	3.18	153	79.5	1.14	0.91	2.43	2.19
1FeNiMoN	21.73	2.34	543.2	58.5	0.97	1.315	2.40	0.140
2FeNiMoN	15.82	-	395.5		0.87	0.88	1.34	2.23
3FeNiMoN	13.25	-	331.2		1.06	0.75	0.223	2.54
4FeNiMoN	20.60	-	315		1.05	1.1	0.83	2.04
5FeNiMoN	8.30	-	207.5		0.88	0.89	0.846	2.34
FeN	15.39	1.82	384.75	45.5	1.24	0.99	2.38	1.43

Table S6. Comparison on catalytic performance for the HER activity of the 1FeNiMoN with literature

Catalyst Name	Electrolyte details	Overpotential at details (cm^{-2})	Current density	Tafel slope (mV dec^{-1})	Ref
$NiMoN_x/C$	0.1 M $HClO_4$	78	onset	35	[23]
$NiSe_2$–NPs/NiMoN–NRs	1.0 M KOH	58 mV	10	68.7	[6]
Pt/Ni-Mo-N-O	Base, acidic, neutral	40.6, 89.5, 101.1	100	30	[24]
NF/Co_4N @ CeO_2	1.0 M KOH	49	10	137.7	[8]
M-CoP/HPFs	0.5 M H_2SO_4 and 1 M KOH	144 and 92	10	52, 71	[25]
W_2N_3/Fe_2N	1.0 M KOH	85.2 and 187.2 mV	10 and 50	56.4	[4]
$NiCo_2O_4/MoO_2$@ALD-NiO	1.0 M KOH	57 and 212	10 and 30	58	[12]
Pt–Ni@NiMoN/NF	1 M KOH	7	10	22.9	[26]

Mo_2N/NiS-5:1	1.0 M KOH	254, 327	10,30	130.08	[14]
Ir-Ni_3N	1 M KOH	7.1, 66.7	1, 10	66.76	[15]
Co-Mo-N	1.0 M KOH	82	10	121	[16]
NNS-d/Ni_2P@NC-NF	1 M KOH	47	10	54.5	[17]
$(Fe_{1-x}Cu_x)_4N$-Cu_2O/CF	1 M KOH	30	10	61	[18]
c-CNT-0.68@TpBpy-Ru	1.0 M KOH solution	112	10	-	[27]
Ni_3N ($Fe_{2-2x}Co_{2x}P$/Ni_3N)	1 M KOH	113	100	-	[21]
NiMoN	1 M KOH	103,227, 293	10,50,100	174	This work
1FeNiMoN	1 M KOH	71, 161, 206	10,50,100	122	This work

Table S7. The overall water electrolysis performance of the 1FeNiMoN//3FeiMoN assembly and its comparison with the recent reports.

Electrode details	Electrolyte details	Cell Voltage (V)	Current density (cm^{-2})	Stability details(hours)	Reference
$NiSe_2$–NPs/NiMoN–NRs	1.0 M KOH	1.51 V	10	50	[6]
NiMoN-NF700	1.0 M KOH	1.49	10	48	[7]
Co_4N@CeO_2	1.0 M KOH	1.56	100		[8]
W_2N_3-10/Fe_2N	1.0 M KOH	1.54 and 1.68 V	10, 50	200	[4]
NiO@$CuCo_2O_4$/MoNi	1.0 M KOH	1.54, 1.71	10,50	200	[11]
$NiCo_2O_4$/MoO_2@ALD-NiO	1.0 M KOH	1.62	10	100	[12]
Co_3N–$Mo_{0.2}$/NF‖Co_3N–$Mo_{0.2}$@FeOOH/NF	1.0 M KOH	1.62	50	12	[13]
Mo_2N/NiS-5:1	1.0 M KOH	1.84	100	100	[14]
Co-Mo-N	1.0 M KOH	1.59	10	16	[16]
NNS-d/Ni_2P@NC-NF	1.0 M KOH	1.49	10	120	[17]
$(Fe_{1-x}Cu_x)_4N$-Cu_2O/CF	1.0 M KOH	1.57	10	80	[18]
Fe_2P/Co_2N	1.0M KOH	1.561	100	120	[28]
Co_2P/Co_4N//NiFe-LDH	1.0 M KOH	1.48	10	50	[29]
1FeNiMoN//3FeiMoN	1 M KOH solution	1.49	10	Multistep for 120 hours	This work

References

1. V. Jayaraman, G. Jang and D.-H. Kim, *Applied Surface Science*, 2024, 159336.
2. N. Sinha and P. Roy, *Inorganic Chemistry*, 2022, **62**, 3349-3357.
3. D. J. Li, U. N. Maiti, J. Lim, D. S. Choi, W. J. Lee, Y. Oh, G. Y. Lee and S. O. Kim, *Nano letters*, 2014, **14**, 1228-1233.
4. T. Kavinkumar, H. Yang, A. T. Sivagurunathan, H. Jeong, J. W. Han and D. H. Kim, *Small*, 2023, DOI: https://doi.org/10.1002/smll.202300963, 2300963.
5. H. Liang, A. N. Gandi, D. H. Anjum, X. Wang, U. Schwingenschlögl and H. N. Alshareef, *Nano letters*, 2016, **16**, 7718-7725.
6. J. Wang, D. T. Tran, K. Chang, S. Prabhakaran, D. H. Kim, N. H. Kim and J. H. Lee, *Energy & Environmental Materials*, 2023, **6**, e12526.
7. B. Chang, J. Yang, Y. Shao, L. Zhang, W. Fan, B. Huang, Y. Wu and X. Hao, *ChemSusChem*, 2018, **11**, 3198-3207.
8. P. Zhou, G. Hai, G. Zhao, R. Li, X. Huang, Y. Lu and G. Wang, *Applied Catalysis B: Environmental*, 2023, **325**, 122364.
9. M. Wang, J. Ren, H. Wang, X. Wang and R. Wang, *Nanoscale*, 2023, **15**, 8217-8224.
10. S. Xie, J. Lin, S. Wang, D. Xie, P. Liu, G. Tan, M. Zhang, D. Ruan, C. Zhen and F. Cheng, *Journal of Power Sources*, 2020, **457**, 228038.
11. T. Kavinkumar, S. Seenivasan, A. T. Sivagurunathan and D.-H. Kim, *Journal of Materials Chemistry A*, 2021, **9**, 21750-21759.
12. T. Kavinkumar, S. Seenivasan, H. Jung, J. W. Han and D.-H. Kim, *Journal of Materials Chemistry A*, 2021, **9**, 21132-21141.
13. W. Huang, Y. Tong, D. Feng, Z. Guo, R. Ye and P. Chen, *ChemSusChem*, 2023, DOI: https://doi.org/10.1002/cssc.202202078, e202202078.
14. Y. Zang, S. Huang, B. Yang, G. Chen, X. Liu and N. Zhang, *Applied Surface Science*, 2023, **611**, 155656.
15. G. Liu, F. Hou, Y. Wang, X. Wang and B. Fang, *Applied Surface Science*, 2023, **637**, 157896.
16. J. Zhu, Q. Du, M. A. Khan, H. Zhao, J. Fang, D. Ye and J. Zhang, *Applied Surface Science*, 2023, **623**, 156989.
17. W.-Z. Chen, M. Zhang, L. Zhang, J. He, Z. Liu and Y.-Q. Wang, *Electrochimica Acta*, 2023, **441**, 141868.
18. M. Wang, X. Zheng, Y. Li, Z. Zou, Y. Ling and Q. Wang, *Chemical Engineering Journal*, 2023, **460**, 141854.
19. K. Dastafkan, S. Wang, C. Rong, Q. Meyer, Y. Li, Q. Zhang and C. Zhao, *Advanced Functional Materials*, 2022, **32**, 2107342.
20. S. F. Hung, Y. Y. Hsu, C. J. Chang, C. S. Hsu, N. T. Suen, T. S. Chan and H. M. Chen, *Advanced Energy Materials*, 2018, **8**, 1701686.

21. W. Ma, D. Li, L. Liao, H. Zhou, F. Zhang, X. Zhou, Y. Mo and F. Yu, *Small*, 2023, DOI: https://doi.org/10.1002/smll.202207082, 2207082.
22. J. Zhu, R. Lu, W. Shi, L. Gong, D. Chen, P. Wang, L. Chen, J. Wu, S. Mu and Y. Zhao, *Energy & Environmental Materials*, 2023, **6**, e12318.
23. W. F. Chen, K. Sasaki, C. Ma, A. I. Frenkel, N. Marinkovic, J. T. Muckerman, Y. Zhu and R. R. Adzic, *Angewandte Chemie International Edition*, 2012, **51**, 6131-6135.
24. W. Yu, Z. Chen, Y. Fu, W. Xiao, B. Dong, Y. Chai, Z. Wu and L. Wang, *Advanced Functional Materials*, 2023, **33**, 2210855.
25. Y. Pan, K. Sun, Y. Lin, X. Cao, Y. Cheng, S. Liu, L. Zeng, W.-C. Cheong, D. Zhao and K. Wu, *Nano energy*, 2019, **56**, 411-419.
26. H. Hu, Z. Zhang, Y. Zhang, T. Thomas, H. Du, K. Huang, J. P. Attfield and M. Yang, *Energy & Environmental Science*, 2023, **16**, 4584-4592.
27. X. Sun, Y. Hu, Y. Fu, J. Yang, D. Song, B. Li, W. Xu and N. Wang, *Small*, 2023, DOI: https://doi.org/10.1002/smll.202305978, 2305978.
28. X. Zhou, Y. Mo, F. Yu, L. Liao, X. Yong, F. Zhang, D. Li, Q. Zhou, T. Sheng and H. Zhou, *Advanced Functional Materials*, 2023, **33**, 2209465.
29. M. Qin, L. Chen, H. Zhang, M. Humayun, Y. Fu, X. Xu, X. Xue and C. Wang, *Chemical Engineering Journal*, 2023, **454**, 140230.